Available online at www.sciencedirect.com
SCIENCE DIRECT®
Surface Science 571 (2004) L311–L318
SURFACE SCIENCE
www.elsevier.com/locate/susc

Surface Science Letters

# Chemisorption of NTCDA on Ag(1 1 1): a NIXSW study including non-dipolar and electron-stimulated effects

J. Stanzel [a], W. Weigand [a], L. Kilian [a], H.L. Meyerheim [b], C. Kumpf [a,*], E. Umbach [a]

[a] *Experimentelle Physik II, Universität Würzburg, Am Hubland, D-97074 Würzburg, Germany*
[b] *Max-Planck Institut für Mikrostrukturphysik, Weinberg 2, D-06120 Halle, Germany*

Received 25 February 2004; accepted for publication 19 July 2004
Available online 19 August 2004

**Abstract**

The adsorption of one monolayer of 1,4,5,8-naphthalene-tetracarboxylicacid-dianhydride (NTCDA) on the Ag(1 1 1)-surface was studied using the normal incidence X-ray standing waves (XSW) technique. Results regarding two key-issues are presented: Most prominent, the precise adsorbate–substrate bonding distance could be evaluated to 3.02 ± 0.02 Å (for the "relaxed monolayer"-structure). This value is significantly smaller than a van der Waals bonding distance and clearly indicates the chemisorptive bonding character. Concordant results were obtained from both O 1s photo- and O KLL Auger electron emission. This was enabled by the development of a data analysis procedure—the second issue addressed—which takes into account non-dipolar contributions to the photoemission as well as electron-stimulated Auger excitations. The latter effect adds a fraction to the total Auger yield being as high as 50% and hence may be important for any XSW study using Auger signals.


*Keywords:* X-ray standing waves; Photoelectron emission; Chemisorption; Aromatics; Silver

## 1. Introduction

Organic molecules of sufficiently small size tend to a pronounced ordering when they are deposited on atomically smooth substrate surfaces. A decisive parameter controlling this behavior is the strength of the bonding between the adsorbate molecules and the substrate. Physisorption or

* Corresponding author. Tel.: +49 9318885127; fax: +49 9318885158.
*E-mail address:* kumpf@physik.uni-wuerzburg.de (C. Kumpf).

0039-6028/$ - see front matter © 2004 Elsevier B.V. All rights reserved.
doi:10.1016/j.susc.2004.07.048

weak chemisorption is a pre-condition for obtaining a long-range ordered overlayer, but within these premises still a very wide spectrum of different adsorption behaviors are found. In the case of a very weak adsorbate–substrate interaction—i.e., physisorption—the molecule-molecule interaction plays the dominant role, and the substrate affects just as a flat support. The growth properties thus often reflect the properties of the organic bulk material. In contrast, for a system with chemisorption the adsorbate–substrate interaction is dominant. In many cases the adsorption is very site-specific which leads to an imposition of the substrate structure upon the adsorbate. While basic structural properties like the size of the unit cell are—in principle—easily detectable by, e.g., low energy electron diffraction or scanning tunnel microscopy, a detailed structural analysis of the adsorption site and the bonding character of large organic adsorbates on inorganic substrates is difficult, and with very few exceptions, no precise geometrical parameters are available so far. However, such data, especially the molecule-substrate distance, would be very useful, on the one hand for a basic understanding of the system, and on the other hand for a comparison with theory or as a starting point for calculations.

For filling this ''knowledge gap'' a very precise structural probe is necessary which allows to measure changes in atomic distances with sub-Ångström resolution. The X-ray standing waves (XSW) technique is well suited for this purpose and gives precise atomic locations of particular species at surfaces, within self-organized monolayers as well as in buried layers (see, e.g., [1,2] and references therein). When atoms or (very) small molecules occupy only one adsorption site, a full site determination can be obtained by triangulation. For multiple-site adsorption additional information from other experimental or theoretical techniques is required. In favorable cases an adsorption site determination is also possible for larger organic molecules, as recently demonstrated for end-capped quaterthiophene (EC4T) adsorbed on Ag(1 1 1) [3]. For larger molecules, especially when not enough structural information is available beforehand, triangulation is impossible, since, e.g., the atomic species may occupy too many different sites. However, in the case of flat molecules which often adsorb in a planar orientation with respect to the substrate, it is at least possible to obtain the vertical molecule-substrate distance, which actually is the most important information for judging the bonding configuration.

In this paper the precise adsorbate–substrate bonding distance is determined for a large, planar, π-conjugated, organic molecule which contains only carbon and oxygen atoms. This result was obtained from normal incidence XSW (NIXSW) measurements on a monolayer of 1,4,5,8-naphthalene-tetracarboxylicacid-dianhydride (NTCDA, $C_{14}O_6H_4$) adsorbed on Ag(1 1 1) in two different, highly-ordered superstructures—a commensurate ''relaxed'' and a more densely packed, incommensurate ''compressed'' structure, consisting of two and four flat-lying molecules per unit cell, respectively (for details see [4]). Methodical difficulties of XSW—non-dipolar effects in the photoemission and secondary excitation channels for the Auger process—are also addressed and a possibility to cope with them is shown.

## 2. The XSW-technique

When the incident X-ray beam fulfills the Bragg condition for an $\mathbf{H} = (hkl)$ Bragg reflection of the substrate single crystal, the incident and Bragg-reflected X-rays interfere to produce a standing wavefield perpendicular to the Bragg planes with the periodicity of the corresponding Bragg plane spacing $d_{\mathbf{H}}$. In an XSW scan the photon energy or the angle of incidence is varied around the Bragg-condition, which shifts the phase of the standing wave-field relative to the (*hkl*)-planes by half of the lattice spacing. Monitoring the X-ray absorption of the atoms of interest during such a scan yields their spatial distribution relative to the Bragg planes with an accuracy of up to $\approx 0.02$ Å. Usually the X-ray absorption is monitored by recording the photoemission, Auger emission or X-ray fluorescence yield, but also photon stimulated ion desorption can be used [5]. In NIXSW the Bragg angle is fixed to 90° while the photon energy is varied. This minimizes the influence of crystal imperfections; therefore the method

becomes applicable to nearly all single crystal substrates.

One of the key aspects in the data evaluation of NIXSW (and XSW) is the way how the X-ray intensity at the location of an atomic species is monitored. Since the recorded absorption yield is proportional to the X-ray intensity at the position of the absorbing atomic species, it can be described by [1,2]

$$I(E) = 1 + R + 2\sqrt{R}F^{\mathbf{H}}\cos\left(\Phi + \frac{2\pi P^{\mathbf{H}}}{d_{\mathbf{H}}}\right), \qquad (1)$$

where $E$ is the photon energy, $I(E)$ the normalized absorption yield, $R = R(E)$ the reflectivity, and $\Phi = \Phi(E)$ the phase of the standing wavefield. The coherent position $P^{\mathbf{H}}$ and the coherent fraction $F^{\mathbf{H}}$ are the structural parameters that can be determined by a fit to the measured data. $P^{\mathbf{H}}$ and $F^{\mathbf{H}}$ are correlated with the position and the distribution, respectively, of the atomic species relative to the $\mathbf{H} = hkl$ plane of the Bragg reflection with lattice spacing $d_{\mathbf{H}}$.

Since the photoemission process can only be induced by photons, it is a direct monitor of the X-ray absorption of surface atoms. However, it has been shown that for light elements like C, N, and O in particular, the usually applied dipole approximation is not sufficient to interpret the NIXSW data correctly [6]. When non-dipolar terms are considered the photoemitted intensity depends on the direction of the incident photon beam, i.e., in general, the incident and reflected beam do not contribute equally to the measured photoelectron yield. Since the ratio of amplitudes of incident and reflected beam varies over the XSW curve (the reflected beam is only present within the Darwin-width of the Bragg reflection), the shape of the XSW photoemission profile is altered by non-dipolar contributions in a non-linear way. This effect can be taken into account by introducing additional correction parameters [7]. For emission from an s-state one obtains [8]

$$I(E) = 1 + R\frac{1+Q}{1-Q} + 2\sqrt{R}F^{\mathbf{H}} \times \frac{(1+Q^2\tan^2\Delta)^{1/2}}{1-Q}\cos\left(\Phi + \Psi + \frac{2\pi P^{\mathbf{H}}}{d_{\mathbf{H}}}\right) \qquad (2)$$

with the non-dipolar parameters $Q$, $\Delta$, and $\Psi = \tan^{-1}(Q\tan\Delta)$ which take the magnetic dipole and the electronic quadrupole contributions to the photoelectron yield into account. For O 1s (and also C 1s) these parameters were measured for incoherent multilayer adsorbates [8,9] and calculated for free atoms [10]. However, since investigations which take non-dipolar effects into account are rare, these parameters are not well established. In particular, no measurement on a coherent monolayer of organic molecules was reported so far.

In order to bypass this difficulty other detection channels like Auger- and fluorescence yield are often considered as an alternative. These processes have an angular distribution which is independent of the photon energy and the direction of incidence, but can also be stimulated by (photo-)electrons emerging from the bulk [11]. The latter effect has to be considered—for light elements in particular—because the electron-induced yield may almost equal the photon-induced one. This aspect is subject of an ongoing discussion in the XSW-community (see, e.g., Refs. [1,12,13] and references therein). Using the system NTCDA/Ag(1 1 1) as an example we will demonstrate that a good agreement between the structural parameters ($P^{\mathbf{H}}, F^{\mathbf{H}}$) derived from the photoemission and the Auger yield, respectively, can *only* be obtained, when non-dipolar contributions *and* electron-induced Auger processes are considered. It should be noted, that the effect of thermal vibration, i.e., a Debye–Waller factor, was neglected in this discussion. This effect directly affects the coherent fraction [14]. However, neglecting the Debye–Waller factor is justified in this case since its influence on the geometric parameters is identical for photoelectron and Auger emission.

## 3. Experimental

The measurements were performed at beamline ID 32 of the European Synchrotron Radiation Facility (ESRF) in Grenoble, France. This beamline, specially designed for surface studies, is equipped with an UHV chamber containing a hemispherical electron analyzer (CHA) ($r$ =

150 mm) with lens, a LEED optics, and facilities for sample preparation. The CHA is placed in the plane of the electric field vector at an angle $\theta = 45°$ with respect to the incident X-ray beam. All experiments and preparations were performed at a base pressure below $5 \times 10^{-10}$ mbar. The Ag(1 1 1) single crystal substrate was prepared by repeated cycles of sputter-cleaning with 500 eV Ar-ions, followed by annealing at temperatures up to 750 K until the surface showed a high structural quality and no detectable contaminations. This was monitored by LEED and XPS. Afterwards the NTCDA monolayer was prepared by evaporating NTCDA from a Knudsen cell. Best results were obtained by deposition of a multilayer followed by subsequent thermal desorption until the compressed and relaxed monolayer, respectively, was observed by LEED (for details see [4]).

After preparation, NIXSW measurements were performed using the Ag(1 1 1) reflection, the normal-incidence Bragg condition of which is fulfilled at a photon energy of 2625 eV. The O 1s photoemission and O KLL Auger yield was recorded. The data and the corresponding best fit are shown in Fig. 1 and discussed below. The figure also contains the bulk absorption profiles, monitored by the secondary background of inelastically scattered Ag-substrate photoelectrons at energies around the O 1s and O KLL peaks, which were used as a calibration for the photon energy and the energetic broadening of the monochromator.

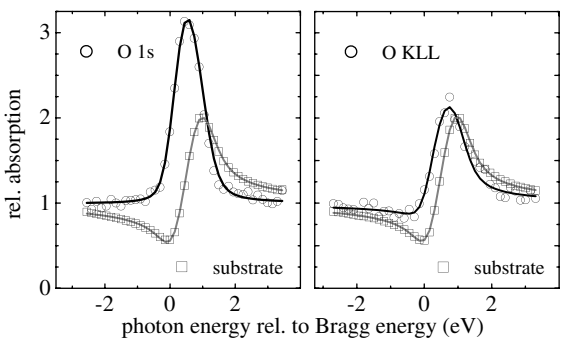


Fig. 1. XSW absorption profiles of a relaxed monolayer NTCDA/Ag(1 1 1), evaluated from the O 1s photoelectron signal (left) and the O KLL Auger-electron yield (right). Additionally substrate signals (background) are shown. The O 1s curve is fitted by Eq. (2), all other data by Eq. (1).

For this purpose the coherent position was fixed to the known bulk spacing $d_{1\,1\,1} = 2.36$ Å during the fit. If treated as a free parameter, structure parameters of $P^{1\,1\,1} = 2.35 \pm 0.02$ Å and $F^{1\,1\,1} = 0.84 \pm 0.03$ were obtained. This confirms that the background of inelastically scattered electrons can be used as a monitor of the bulk absorption profile [2]. The absorption profiles were fit by a code [3] which was modified in order to consider non-dipolar effects. During the measurements no changes in the XPS spectra were observed that would indicate radiation damage in the organic layer.

## 4. Results

### 4.1. Correct treatment of PES and Auger XSW data

The results of the NIXSW measurements on a relaxed monolayer of NTCDA on Ag(1 1 1) are shown in Fig. 1. A fit to the O 1s absorption profile in dipol-approximation (use of Eq. (1)) yields a coherent position $P^{1\,1\,1}_{\mathrm{O\,1s}} = 3.01(2)$ Å and a coherent fraction of $F^{1\,1\,1}_{\mathrm{O\,1s}} = 1.05(16)$. The latter value indicates, that non-dipolar effects cannot be neglected. Employing Eq. (2) with the non-dipolar parameters evaluated by Lee et al. [8] ($Q = 0.26$, $\Delta = -0.33$) results in values of $P^{1\,1\,1}_{\mathrm{O\,1s}} = 3.02(2)$ Å and $F^{1\,1\,1}_{\mathrm{O\,1s}} = 0.59(11)$ (see also Table 1), i.e., the coherent fraction is changed significantly whereas the coherent position is hardly affected.

When the O KLL Auger yield is used, a completely different result is obtained, $P^{1\,1\,1}_{\mathrm{O\,KLL}} = 2.60(3)$ Å and $F^{1\,1\,1}_{\mathrm{O\,KLL}} = 0.46(5)$. In Fig. 2 (left Argand diagram) the positional parameters are shown as complex (position-) vectors $F^{\mathbf{H}} \cdot \exp(2\pi i P^{\mathbf{H}}/d_{\mathbf{H}})$. Their lengths and phase-angles correspond to the coherent fraction $F^{\mathbf{H}}$ and the coherent position $P^{\mathbf{H}}$, respectively. The vectors labelled 'O 1s' and '$(\mathrm{O\ 1s})_c$' represent the O 1s result with and without the use of non-dipolar corrections, respectively. Even after the correction of the O 1s result there is no agreement with the Auger data ('O KLL'). However, when the O KLL result is corrected as described below, the resulting vector '$(\mathrm{O\ KLL})_c$' does agree with the (corrected)

Table 1
Structural parameters obtained from O 1s- and O KLL-NIXSW measurements

| ML | | O 1s | O 1s corr.[a] | O KLL | O KLL corr.[b] |
|---|---|---|---|---|---|
| Relax. | $P^{111}$ (Å) | 3.01(2) | 3.02(2) | 2.60(3) | 3.03 |
| | $F^{111}$ | 1.05(16) | 0.59(11) | 0.46(5) | 0.56 |
| Comp. | $P^{111}$ (Å) | 3.08(3) | 3.12(3) | 2.64(3) | 3.06 |
| | $F^{111}$ | 0.98(3) | 0.46(4) | 0.45(4) | 0.64 |

[a] Non-dipolar parameters: $Q = 0.26$, $\Delta = -0.33$ [8].
[b] Electron-induced Auger transitions ($a = 50\%$) considered.

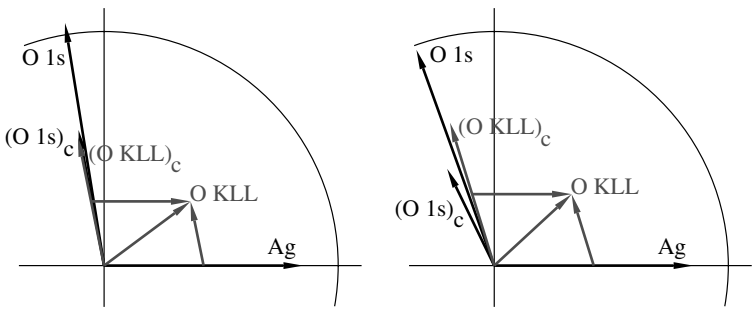


Fig. 2. Argand diagram for a relaxed (left) and a compressed (right) monolayer of NTCDA/Ag(111). Measured and corrected position vectors evaluated from the O KLL (grey) and the O 1s (black) XSW signal are shown. The measured O KLL position vector consists of adsorbate-like and bulk-like ('Ag') contributions. For the correction of the O KLL result an electron-induced portion of $a = 50\%$ is assumed. Details are explained in the text.

photoemission-XSW result. The right part of Fig. 2 shows that the results obtained for the compressed monolayer structure are quite similar to those for the relaxed monolayer (see also Table 1).

What is the origin of the discrepancy between O 1s and O KLL XSW results? A core hole can be excited by photons and also by electrons, for the subsequent Auger decay this makes (nearly) no difference. Therefore the O KLL-XSW signal has two contributions, one originating from the photon-excitation which carries the structural information from the oxygen atoms in the overlayer, the other originating from the excitation by escape-electrons from the bulk. The latter contribution is mainly caused by (inelastically scattered) photoelectrons from the Ag substrate, which therefore yields the structural signature of Ag bulk-atoms in an XSW-scan. Thus, the measured O KLL position vector is the normalized sum of two vectors: $\vec{O}_{KLL} = a \cdot \vec{Ag} + (1 - a) \cdot \vec{O}$, where $a$ is the fraction of the electron induced Auger transitions, $\vec{O}$ and $\vec{Ag}$ are the position vectors of the oxygen atoms (in the overlayer) and Ag atoms (in the bulk), respectively. Since the bulk structure is usually well known, $\vec{Ag}$ can be calculated (and also measured) and thus the real Auger signal $\vec{O}$ can be evaluated, if the electron-induced portion $a$ is known. Even though this aspect has already been addressed before (see, e.g., [12]) it is widely ignored in recent publications. One exception is a recent paper by Pacilé et al. [13]. In the present example, a value in the range of $a = 50\%$, which is a result of a rough fit to the data, gives a good agreement with the corrected photoemission results (see Fig. 2). We will argue in Section 4.3, that this fit result appears to be realistic.

We would like to note that the excellent agreement between the corrected O 1s and O KLL vectors in the Argand diagram for both the relaxed and the compressed adsorption states is a strong indication that the presented approach is correct since only one parameter, $a$, is required to bring

the four parameters of the Argand vectors ($P^{\mathbf{H}}$ and $F^{\mathbf{H}}$ for both states) into agreement with the corresponding photoemission vectors. We further note that the contribution of electron-excitation by substrate photoemission to the Auger emission from the adsorbate is particularly high for light-atom adsorbates since, e.g., in the present case, the kinetic energy of the substrate photoelectrons (≈2250 eV for Ag 3d and ≈2050/2020 eV for Ag 3p) is about four times higher at the Bragg energy than the binding energy of the O 1s level (534 eV), leading to a maximum of the cross-section of electron excitation (see also Fig. 3, left).

### 4.2. Chemisorption of NTCDA/Ag(1 1 1)

In Table 1 the structural results are summarized. In the case of the relaxed monolayer structure an excellent agreement can be obtained for O KLL and O 1s results. The adsorbate–substrate distance is found to be 3.02(2) Å, a value which lies significantly below the expected distance of 3.38 Å for a van der Waals-like bonding [15]. The bond length for a direct covalent Ag–O bond (e.g., after dissociation) would be 2.21 Å. These numbers prove, that the NTCDA molecule is not physisorbed on Ag(1 1 1) (i.e., by a van der Waals-type coupling) but rather that the adsorbate–substrate bonding has a chemisorptive character. For the compressed monolayer a similar behavior is found, even though the agreement between the O KLL and O 1s results is not as good as for the relaxed monolayer. The average adsorbate–substrate distance is 3.09(4) Å, and hence slightly larger than for the relaxed monolayer. This finding might be due to a larger distorsion of the molecule in this adsorbate state as compared to the relaxed state. The occurrence of distortion upon chemisorption is rather likely as shown previously for the system EC4T on Ag(1 1 1) [16].

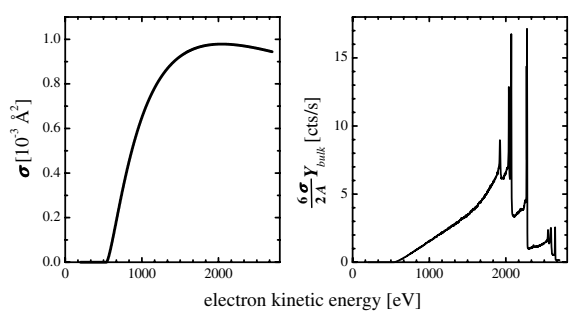


Fig. 3. The electron impact cross-section $\sigma$ (left) [17] and the integrand of Eq. (3) (right) are plotted versus the electron kinetic energy.

### 4.3. Electron-stimulated Auger decays

Finally we show in the following, that the fraction of electron-induced Auger processes in the NTCDA overlayer is indeed in the range of 50%, as experimentally derived from the correction of the O KLL XSW results above. The ratio of the total *electron*-induced Auger yield $I_{\mathrm{O\,KLL,e^-}}$ to the *photon*-induced fraction $I_{\mathrm{O\,KLL},h\nu}$ can be written as

$$\frac{I_{\mathrm{O\,KLL,e^-}}}{I_{\mathrm{O\,KLL},h\nu}} = \frac{\int \frac{6\sigma(E_k)}{A}\,\frac{1}{2} I_{\mathrm{bulk}}(E_k)\,\mathrm{d}E_k}{I_{\mathrm{O\,KLL},h\nu}} = \frac{\int \frac{6\sigma(E_k)}{A}\,\frac{1}{2} Y_{\mathrm{bulk}}(E_k)\,\mathrm{d}E_k}{cY_{\mathrm{O\,1s}}} \approx 0.43, \qquad (3)$$

where $E_k$ is the electron kinetic energy, $I_{\mathrm{bulk}}(E_k)$ is the yield of electrons emerging from the substrate, $A = 86.8\,\text{Å}^2$ is the area of a NTCDA molecule in the relaxed monolayer-structure, which is known from LEED and STM investigations [4], and $\sigma(E_k)$ is the electron impact ionization cross-section (see Fig. 3, left). The latter is calculated using the formula of Gryzinski [17], which yields similar results as alternative approaches [18]. The factor 6 considers the number of oxygen atoms per molecule.

The key parameter in Eq. (3) is the yield of secondary electrons in the adsorbate layer $I_{\mathrm{bulk}}(E_k)$ originating from the Ag substrate and its energy distribution. Since it mainly consists of inelastically scattered electrons an isotropic angular distribution is assumed. A factor of $\frac{1}{2}$ must hence be considered since only the electrons emitted towards the surface pass the adsorbate layer, i.e., only half of the bulk-electrons possibly induce an Auger emission from the layer. The second equal sign in Eq. (3) is valid since the ratio of $I_{\mathrm{bulk}}(E_k)$ to $I_{\mathrm{O\,KLL},h\nu}$ can be replaced by the ratio of the corresponding measured quantities: $Y_{\mathrm{bulk}}(E_k)$, obtained by a survey scan of the clean Ag(1 1 1)

sample, represents the total electron yield emerging from the bulk. $Y_{O\,1s}$ is the integral intensity of the O 1s photoemission peak of a monolayer of NTCDA/Ag(1 1 1) and can be used as a measure of the photon-induced O KLL Auger yield since a decay of the core hole via fluorescence can be neglected for light elements. Both measured electron yields were normalized to the incident photon intensity $I_0$. Note that $I_{bulk}(E_k)$ and $I_{O\,KLL,h\nu}$ represent *total* electron yields, i.e., emission into all directions ($4\pi$-emission) while $Y_{bulk}(E_k)$ and $Y_{O\,1s}$ consider only emission into the acceptance cone of the analyzer since these are measured quantities. Hence, an additional factor $c$ has to be introduced to take into account that the O 1s photoemission process is not isotropic. From geometric considerations, the acceptance angle of the detector, and the angular distribution of the photoelectron emission, this factor can be roughly calculated to $c = 0.6$. It is mentioned that a possible (kinetic) energy-dependence of the detector sensitivity due to a varying detector transmission is neglected since it does not play a significant role.

The right part of Fig. 3 shows the energy dependence of the integrand in Eq. (3) as product of the electron impact ionization cross-section and the electron yield emerging from the substrate, normalized to the area of the molecule. Integration and comparison with $I_{O\,KLL,h\nu}$ results in an electron stimulated portion of the total Auger yield of 30% (corresponding to the ratio $I_{O\,KLL,e^-}/I_{O\,KLL,h\nu} = 0.43$, see Eq. (3)). Note that this rough estimate is a lower limit, because inelastic scattering processes from bulk electrons which pass the adsorbate layer at a grazing angle and hence experience a much larger scattering and O 1s ionization probability are largely underestimated by using Eq. (3). We simulated this effect by a simple geometrical model and found that the actual electron stimulated fraction of the total Auger yield is 42%. Therefore the value of 50% derived from the NIXSW results appears to be realistic.

## 5. Summary

In summary, we have demonstrated that the NIXSW method is able to provide consistent results from photoemission *and* Auger yields also for large organic molecules with only light elements, when non-dipolar contributions to the photoemission process and the electron-stimulated portion of the Auger yield are considered. The results actually prove that by using an (uncorrected) Auger emission as NIXSW monitor much larger errors may be introduced as compared to the neglect of non-dipolar contributions in photoemission, if the data are not properly corrected for electron-induced Auger contributions due to bulk photoemission. The amount of electron-stimulated Auger excitations is estimated to 50% of the total Auger yield in the present case. This approach can also be considered to be a proof for the non-dipolar parameters necessary to correct the photoemission data.

For the case of NTCDA on Ag(1 1 1) adsorbate–substrate bonding distances of 3.02(2) Å for the relaxed monolayer and 3.09(4) Å for the compressed monolayer were found which indicate a covalent character of the molecular adsorption.

## Acknowledgments

The authors acknowledge financial and experimental support by the ESRF, Grenoble. In particular we would like to thank T.-L. Lee, B.C.C. Cowie and J. Zegenhagen for fruitful discussions and their support during the beamtime. One of us (E.U.) would like to thank the Fonds der Chemischen Industrie for financial support.

## References

[1] J. Zegenhagen, Surf. Sci. Rep. 18 (1993) 202;
D.P. Woodruff, Prog. Surf. Sci. 57 (1998) 1.
[2] R.G. Jones, A.S.Y. Chan, M.G. Roper, M.P. Skegg, I.G. Shuttleworth, C.J. Fisher, G.J. Jackson, J.J. Lee, D.P. Woodruff, N.K. Singh, B.C.C. Cowie, J. Phys.: Condens. Matter 14 (2002) 4059.
[3] L. Kilian, W. Weigand, E. Umbach, A. Langner, M. Sokolowski, H.L. Meyerheim, H. Maltor, B.C.C. Cowie, T. Lee, P. Bauerle, Phys. Rev. B 66 (2002) 075412.
[4] U. Stahl, D. Gador, A. Soukopp, R. Fink, E. Umbach, Surf. Sci. 414 (1998) 423;
R. Fink, D. Gador, U. Stahl, Y. Zou, E. Umbach, Phys.

Rev. B 60 (1999) 2818;
L. Kilian, Dissertation, University of Würzburg, 2002.
[5] J. Falta, A. Hille, T. Schmidt, G. Materlik, Surf. Sci. 436 (1999) L677.
[6] C.J. Fisher, R. Ithin, R.G. Jones, G.J. Jackson, D.P. Woodruff, B.C.C. Cowie, J. Phys.: Condens. Matter 10 (1998) L623.
[7] I.A. Vartanyants, J. Zegenhagen, Solid State Commun. 113 (2000) 299;
I.A. Vartanyants, J. Zegenhagen, Solid State Commun. 115 (2000) 161 (Erratum).
[8] J.J. Lee, C.J. Fisher, D.P. Woodruff, M.G. Roper, R.G. Jones, B.C.C. Cowie, Surf. Sci. 494 (2001) 166.
[9] G.J. Jackson, B.C.C. Cowie, D.P. Woodruff, R.G. Jones, M.S. Kariapper, C. Fisher, A.S.Y. Chan, M. Butterfield, Phys. Rev. Lett. 84 (2000) 2346;
F. Schreiber, K.A. Ritley, I.A. Vartanyants, H. Dosch, J. Zegenhagen, B.C.C. Cowie, Surf. Sci. 486 (2001) L519.
[10] M.B. Trzhaskovskaya, V.I. Nefedov, V.G. Yarzhemsky, At. Data Nucl. Data Tables 77 (2001) 97.
[11] A.G. Shard, B.C.C. Cowie, J. Phys.: Condens. Matter 10 (1998) L69.
[12] J.C. Woicik, T. Kendelewicz, K.E. Miyano, P.L. Cowan, C.E. Bouldin, B.A. Karlin, P. Pianetta, W.E. Spicer, Phys. Rev. Lett. 68 (1992) 341.
[13] D. Pacilé, M. Papagno, A. Cupolillo, G. Chiarello, L. Papagno, J. Electron. Spectrosc. 135 (2004) 201.
[14] N. Hertel, G. Materlik, J. Zegenhagen, Z. Phys. B: Condens. Matter 58 (1985) 199.
[15] A. Bondi, J. Phys. Chem. 68 (1964) 441.
[16] H.L. Meyerheim, T. Gloege, M. Sokolowski, E. Umbach, P. Bäuerle, Europhys. Lett. 52 (2000) 144.
[17] M. Gryzinski, Phys. Rev. 138 (1965) A336.
[18] M.P. Seah, in: D. Briggs, M.P. Seah (Eds.), Practical Surface Analysis, vol. 1, second ed., J. Wiley & Sons, Chichester, 1990, p. 201.